ISSN 1846-6168 (Print), ISSN 1848-5588 (Online)
https://doi.org/10.31803/tg-20240708150316

Original scientific paper
Received: 2024-07-08, Accepted: 2025-04-15

Low-Cost Attitude Determination Using Two GPS Antennas and IMU Data

Habib Kanberoğlu (Habib Ghanbarpourasl)*, Mukaddes Bolat

Abstract: This study explores methods for precise attitude estimation using carrier phases within global positioning systems (GPS). Carrier phase data is preferred over pseudorange data for short baseline distances due to its lower noise levels. However, resolving ambiguities through integer ambiguity resolution methods is essential for effectively utilizing carrier phases. One widely adopted approach, the LAMBDA method, is introduced, alongside a solution tailored for low-cost GPS systems and receivers with higher error. The novel method primarily focuses on utilizing only the fractional parts of the carrier phases while integrating constraints such as pitch and baseline constraints to enhance ambiguity detection accuracy. Comparative analysis with the LAMBDA approach demonstrates that the proposed method achieves remarkable accuracy, even in environments characterized by multipath interference.

Keywords: Attitude determination; GPS carrier phase; Integer ambiguity; LAMBDA method

1 INTRODUCTION

Satellite-based global positioning systems (GPS) boast diverse applications, ranging from providing precise navigation solutions for aircraft and maritime vessels to facilitating kinematic positioning across varying scales, from short distances to several kilometers. Moreover, rotation estimation becomes attainable with the appropriate configuration of GPS antennas within a unified system. GPS antennas are used to detect yaw, pitch, and roll by using measurements representing the distance between the receiver and satellites. Pseudorange measurements, which involve measuring the time it takes for the satellite signal to travel from the satellite to the receiver, can provide distance measurements. However, they are subject to errors caused by factors such as atmospheric delays and receiver clock errors. Carrier phase measurements, on the other hand, offer much higher precision because they directly measure the phase of the carrier wave. While carrier phase measurements offer higher precision, they pose the challenge of resolving the integer ambiguity [1]. The integer ambiguity arises because the receiver cannot directly determine how many complete cycles the carrier wave has traveled [2]. Instead, it measures the total phase change since the signal was transmitted. This total phase change includes both the fractional part (which can be accurately measured) and the integer part (which cannot be directly measured). Various methods have been developed to resolve these integer ambiguities and enable accurate positioning and rotation using carrier phase measurements in GPS applications.

These methods are typically categorized into two main groups. Motion-based techniques require the accumulation of data over a specific period during which significant changes occur either in the visible GPS constellation or in the observable platform rotations. Conversely, search-based methods rely on single epoch measurements to identify the most probable ambiguity combination, acknowledging that noise levels may sometimes lead to incorrect ambiguity identification [3].

Some of the earliest applied integer ambiguity resolution methods are the LSAST [4], FASF [5] and AFM [6], methods. LSAST and FASF are search-based methods that rely on sequential least squares estimation and operate under the assumption of normally distributed errors within a properly defined ambiguity search space. As stated by [7], these methods always include the correct set of ambiguities within the search space and obtain the least squares solution. D. Kim and R. B. Langley applied the OMEGA method by modifying the LSAST method to follow a more efficient process. It adopts two search space reduction processes (a scaling and a scanning process) to transform the search space and filter ambiguity candidates at multiple search levels. To achieve maximum efficiency, an optimization procedure is applied in a closed form before the search-validation step, determining parameters that minimize candidates under specific conditions [8].

On the other hand, the AFM method is a motion-based technique that utilizes only the fractional components of instantaneous carrier phase measurements. As a result, the ambiguity function values remain unaffected by full-cycle changes or cycle slips in the carrier phase. The adaptive nature inherent in AFM is characterized by a nonlinear and highly complex structure. Consequently, the process of searching for its maximum value demands a significant amount of computational capacity, creating a bottleneck in GPS attitude determination [9]. To reduce the computational burden, some enhanced AFM methods have been developed. Ref. [10] aims to minimize the number of grid points that need to be tested and determine the optimal search step size while [11] focuses on minimizing the number of test points to reduce computational load.

The ARCE method, or Ambiguity Resolution with Constraint Equation, is a sophisticated motion-based technique utilized to establish the connection between integer ambiguities. This correlation can be established separately from the user's location. These ambiguities consist of three distinct elements that are utilized to derive the user's position. Upon determining the independent elements, the remaining dependent elements can be calculated using the constraint equation. This technique provides a direct method for determining the dependent elements without requiring knowledge of the user's location. Furthermore, the

covariance information obtained from these ambiguities can be used as an additional criterion for rejection [12].

The aforementioned techniques exhibit both merits and demerits. Among the primary challenges encountered with integer ambiguity resolution methods are the computational overhead and intricate structures. These limitations often translate into inaccuracies within real-time attitude determination applications. Presently, the widely adopted LAMBDA method effectively mitigates this computational burden. LAMBDA method [13], which stands for "Least-squares Ambiguity Decorrelation Adjustment". LAMBDA involves a two-step process to compute integer least squares (ILS) ambiguity estimates. In the first step, the LAMBDA method employs Z-transformation to decorrelate ambiguities. This decorrelation step is crucial as it facilitates the effective search for the integer candidate solving the integer minimization problem. The second step in the LAMBDA method involves the search process, which is facilitated by the elimination of correlations obtained in the first step [14]. Test results for rotation estimation using the LAMBDA method can be found in [15].To enhance the success rate of the LAMBDA method, several baseline-constrained versions have been proposed [16–18]. While the original formulation of the LAMBDA method is applicable to both unconstrained and linearly constrained GNSS models, its baseline-constrained version, MLAMBDA [19], can be applied to second-order constrained GNSS models as well [2].

In this study, as observed, the LAMBDA method yields superior results in expensive GPS devices and suitable environments, while its accuracy diminishes in cheaper GPS devices and multipath environments. It is well known that other search-based and motion-based methods struggle with computational overhead and complex structures, as mentioned above. This study aims to achieve low-error attitude estimation even in multipath environments. To accomplish this, a New method has been developed, incorporating constraints such as baseline constraint and rotation constraint to accurately determine integer ambiguities.

1.1 GNNS Observation Model

It is important to note that there are multiple sources of error in carrier phase and pseudorange measurements, including ionospheric, tropospheric, satellite clock, receiver clock, and multipath errors. The undifferenced code and carrier phase measurements can be modeled as [20]:

$$p_a^s = \rho_a^s + c(dt_a - dt^s) + I_a^s + T_a^s + M_{a,P}^s + \varepsilon_{a,P}^s \phi_a^s \quad (1)$$

$$\phi_a^s = \rho_a^s + c(dt_a - dt^s) + I_a^s + T_a^s + M_{a,\phi}^s + \varepsilon_{a,\phi}^s + \lambda N_a^s \quad (2)$$

Where superscript s stays for representation of s-th satellite, and subscript a stays for a-th receiver. p_a^s and ϕ_a^s are the pseudorange and carrier phase measurements from s-th satellite to a-th receiver, ρ_a^s is the geometric range, dt_a and dt^s are clock biases of the a-th receiver and the s-th satellite, I_a^s and T_a^s are the ionospheric and trophospheric delay between the s-th satellite and the a-th receiver, $M_{a,P}^s$ and $M_{a,\phi}^s$ are the multi-path errors for the code and carrier phase of the a-th receiver, $\varepsilon_{a,P}^s$ and $\varepsilon_{a,\phi}^s$ are the errors that cannot be modeled and are assumed to be white Gaussian noises, λ is the wavelength and N_r^s is the unknown integer ambiguity.

To elimination the clock difference of satellites, we can compare signals from two antennas. Atmosphere and satellite errors are eliminated by single difference of measurements between receivers for short baselines. After a single difference (SD) between receivers *a* and *b*, the model can be written as:

$$\Delta p_{rb}^s = p_r^s - p_{rb}^s = \Delta\rho_{rb}^s + c(\Delta dt_{rb}) + M_{rb,P}^s + \varepsilon_{rb,P}^s \quad (3)$$

$$\Delta\phi_{rb}^s = \phi_r^s - \phi_b^s = \Delta\rho_{rb}^s + c(\Delta dt_{rb}) + M_{rb,\phi}^s + \varepsilon_{rb,\phi}^s - \lambda\Delta N_{rb}^s \quad (4)$$

Where Δp_{ab}^s and $\Delta\phi_{ab}^s$ represents the SD pseudorange and carrier phase measurements between a-th and b-th receiver respectively. Moreover, to eliminate receiver's clock biases, we perform double difference between two satellites measurements, resulting in the following double differenced (DD) measurements

$$\nabla\Delta p_{rb}^{sk} = \Delta\rho_{rb}^s - \Delta\rho_{rb}^k = \Delta\rho_{rb}^{sk} + M_{rb,P}^{sk} + \varepsilon_{rb,P}^{sk} \quad (5)$$

$$\nabla\Delta\phi_{rb}^{sk} = \Delta\rho_{rb}^s - \Delta\rho_{rb}^k = \Delta\rho_{rb}^{sk} + M_{rb,\phi}^{sk} + \varepsilon_{rb,\phi}^{sk} - \lambda\Delta N_{rb}^{sk} \quad (6)$$

Where, $\nabla\Delta p_{ab}^{sk}$ and $\nabla\Delta\phi_{ab}^{sk}$ represent the DD pseudorange and carrier phase measurements between the a-th and b-th receivers, and the s-th and k-th satellites. The linearized observation equation for both Eqs. (5) and (6) can be written in the following form [14]:

$$y = Aa + Br^n + \eta \quad (7)$$

Where y is the DD pseudorange and carrier phase measurements. The vector a is the DD carrier phase ambiguity which is an integer vector. Vector r^n is the baseline vector in local navigation frame which is represented by its three component *x*, *y* and *z*. A is a constant matrix, and matrix B is function of satellite unit vectors and wavelength. The vectors and matrices in Eq. (7) can be expressed as:

$$y=\begin{bmatrix}\nabla\Delta p_{rb}^{s1}-\nabla\Delta p_{rb}^{s2}\\ \nabla\Delta p_{rb}^{s1}-\nabla\Delta p_{rb}^{s3}\\ \vdots\\ \nabla\Delta p_{rb}^{s1}-\nabla\Delta p_{rb}^{sn}\\ \nabla\Delta \phi_{rb}^{s1}-\nabla\Delta \phi_{rb}^{s2}\\ \nabla\Delta \phi_{rb}^{s1}-\nabla\Delta \phi_{rb}^{s3}\\ \vdots\\ \nabla\Delta \phi_{rb}^{s1}-\nabla\Delta \phi_{rb}^{sn}\end{bmatrix} B=\begin{bmatrix}(e^{s1}-e^{s2})^T\\ (e^{s1}-e^{s3})^T\\ \vdots\\ (e^{s1}-e^{sn})^T\\ \frac{(e^{s1}-e^{s2})^T}{\lambda}\\ \frac{(e^{s1}-e^{s3})^T}{\lambda}\\ \vdots\\ \frac{(e^{s1}-e^{sn})^T}{\lambda}\end{bmatrix} A=\begin{bmatrix}0 & \cdots & 0\\ \vdots & \ddots & \vdots\\ 0 & \cdots & 0\\ 1 & \cdots & 0\\ \vdots & \ddots & \vdots\\ 0 & \cdots & 1\end{bmatrix} r^n=\begin{bmatrix}b_x\\ b_y\\ b_z\end{bmatrix} a=\begin{bmatrix}a^{s1}-a^{s2}\\ a^{s1}-a^{s3}\\ \vdots\\ a^{s1}-a^{sn}\end{bmatrix} \eta=\begin{bmatrix}\eta^{s1}-\eta^{s2}\\ \eta^{s1}-\eta^{s3}\\ \vdots\\ \eta^{s1}-\eta^{sn}\end{bmatrix}$$

Where n is the number of visible satellites. If there are n visible satellites, there are $n-1$ DD carrier phases and pseudoranges when the satellite 1 is selected as the pivot satellite. η is supposed to be white and Gaussian with zero mean and covariance Q_y. The matrix A consists of two parts: the first part is associated with the pseudorange measurements, while the second part which is represented by a unit matrix, is associated with carrier phase measurements. This choice of a unit matrix reflects the fact that carrier phase measurements inherently contain integer ambiguity.

The aim of this study is to find the integer ambiguity vector a and estimate the relative position vector between antennas by fixing the carrier phases, and then attitude determination will be applicable.

2 ATTITUDE DETERMINATION

The positions and distances of the antennas in the body frame are shown in Fig. 1. The position of the antennas are fixed and when the antenna 1 is taken as a reference antenna, the position vectors of antenna 2 and antenna 3 with respect to antenna 1 is:

$$r_2^b=\begin{bmatrix}L_{12}\\ 0\\ 0\end{bmatrix}\ r_3^b=\begin{bmatrix}L_{13}\cos\alpha\\ L_{13}\sin\alpha\\ 0\end{bmatrix} \tag{8}$$

Where L12 is the distance between antenna 1 and antenna 2, and L13 is the distance between antenna 1 and antenna 3, α is the angle between antenna 1, antenna 2 and antenna 3, r_2^b and r_3^b are the position of antenna 2 and 3 with respect to the antenna 1 in body frame.

The rotation matrix between body and navigation frame is defined as [21]:

$$C_b^n=\begin{bmatrix}\cos\psi & -\sin\psi & 0\\ \cos\psi & \sin\psi & 0\\ 0 & 0 & 1\end{bmatrix}\begin{bmatrix}\cos\theta & 0 & \sin\theta\\ 0 & 1 & 0\\ -\sin\theta & 0 & \cos\theta\end{bmatrix}\begin{bmatrix}1 & 0 & 0\\ 0 & \cos\varphi & -\sin\varphi\\ 0 & 0 & \cos\varphi\end{bmatrix}=C_1^nC_2^1C_b^2 \tag{9}$$

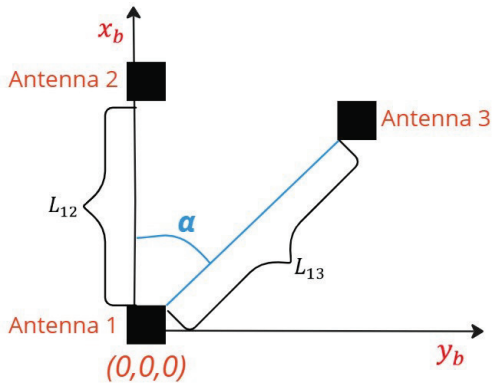

Figure 1 Position of antennas in the body reference system.

Where ψ, θ, and ϕ are the heading, pitch, and roll angles of the body frame with respect to the navigation frame, respectively. With reference to Fig. 1, relation between r^b and $r^n$is:

$$r_2^n=C_b^nb_2,\ r_2^b=\begin{bmatrix}L_{12}\\ 0\\ 0\end{bmatrix},\ r_2^n=\begin{bmatrix}x_2\\ y_2\\ z_2\end{bmatrix} \tag{10}$$

By substituting Eq. (9) into Eq. (10), one can write:

$$\begin{bmatrix}L_{12}\cos\psi\cos\theta\\ L_{12}\sin\psi\cos\theta\\ -L_{12}\sin\theta\end{bmatrix}=\begin{bmatrix}x_2\\ y_2\\ z_2\end{bmatrix} \tag{11}$$

From Eq. (11), the heading and pitch angles are found as follows:

$$\psi=\tan^{-1}\left(\frac{y_2}{x_2}\right) \tag{12}$$

$$\theta=\sin^{-1}\left(\frac{-z_2}{L_{12}}\right) \tag{13}$$

When we are using two antennas with configuration showed in Fig. 1, just heading and pitch angles are observable. If three antennas are positioned, then it becomes possible to estimate roll, pitch, and heading angles by three GPS antennas. If the rotation angles are known from Eq. (12) and Eq. (13), one can write:

$$r_3^b = \begin{bmatrix} L_{13}\cos\alpha \\ L_{13}\sin\alpha \\ 0 \end{bmatrix},\ r_2^3 = C_1^2 C_n^1 r_3^n \tag{14}$$

Then r_3^2 and r_3^b are known vectors, then:

$$r_3^b = C_2^b r_3^2,\ r_3^n = \begin{bmatrix} x_3 \\ y_3 \\ z_3 \end{bmatrix},\ r_3^b = \begin{bmatrix} L_{13}\cos\alpha \\ L_{13}\cos\varphi\sin\alpha \\ L_{13}\sin\psi\sin\alpha \end{bmatrix} \tag{15}$$

By comparing equivalent components, it resulted as:

$$\phi = \tan^{-1}\left(\frac{z_3}{y_3}\right) \tag{16}$$

Algebraic method is a classic method for attitude determination [22]. If two or more vectors are known in both frames, the rotation matrix between these frames can be found. For example, let r_1^b and r_2^b be two known vectors in the body frame. The equivalent of these vectors in the navigation frame are r_1^n and r_2^n. The transformation matrix C_b^n is calculated as follows:

$$N = C_b^N B \tag{17}$$

$$B = [r_1^b \quad r_2^b \quad r_1^b \times r_2^b],\ N = [r_1^n \quad r_2^n \quad r_1^n \times r_2^n] \tag{18}$$

Using least squares (LS) method, the rotation matrix can be estimated as:

$$C_B^N = (NB^T BB^T)^{-1} \tag{19}$$

After these calculations, the transformation matrix may not remain orthonormal. To make it orthonormal [23]:

$$\hat{C}_b^n = C_b^n (chol((C_b^n)^T C_b^n)^{-1} \tag{20}$$

chol is the 'cholesky factorization' of a matrix. After calculation of transformation matrix, the roll, heading, and pitch angles can be calculated as follows:

$$\emptyset = \tan^{-1}\left(\frac{\hat{C}_b^n(3,2)}{\hat{C}_b^n(3,3)}\right) \tag{21}$$

$$\psi = \tan^{-1}\left(\frac{\hat{C}_b^n(2,1)}{\hat{C}_b^n(1,1)}\right) \tag{22}$$

3 THE INTEGER AMBIGUITY RESOLUTION METHODS

In this section, the LAMBDA method, one of the integer ambiguity resolution methods that we mentioned in the introduction section, and our method are introduced.

3.1 LAMBDA

The LAMBDA Method is a well-known and widely used method for resolving integer ambiguities in carrier phase measurements. In the LAMBDA method, the least squares principle is often used to estimate the baseline and integer DD ambiguities [14]:

$$\min_{a,b} \| y - Aa - Bb \|_{Q_y}^2,\quad a \in Z^n, b \in R^p \tag{23}$$

Where $\|e\|_A^2$ is the second norm of a vector with weighting matrix A as:

$$\|e\|_A^2 = (e)^T A^{-1}(e) \tag{24}$$

Q_y is the covariance matrix of GNSS observations. These types of least squares problems are called integer least squares (ILS) and differ from standard least squares due to the integer behavior of (a ∈ Zn) [19]. The LAMBDA Method involves three main steps: float solution, integer ambiguity estimation, and fixed solution. In the float solution step, the integer aspect of the ambiguities a is ignored, and floating point solutions of a and the baseline vector r^n are calculated, and suppose the least squares solution of the problem defined by Eq. (7) is:

$$\begin{bmatrix} \hat{b} \\ \hat{a} \end{bmatrix}, \begin{bmatrix} Q_{\hat{b}\hat{b}} & Q_{\hat{b}\hat{a}} \\ Q_{\hat{a}\hat{b}} & Q_{\hat{a}\hat{a}} \end{bmatrix} \tag{25}$$

Where $\hat{a}$ and $\hat{b}$ are float solutions, $Q_{\hat{b}\hat{b}}$ and $Q_{\hat{a}\hat{a}}$ are covariance, and $Q_{\hat{a}\hat{b}}$ is cross-covariance between a and b.

In the integer ambiguity estimation step, the float solution $\hat{a}$ is used to calculate the corresponding integer ambiguity estimate:

$$\check{a} = S(\hat{a}) \tag{26}$$

Where $S: R^n \rightarrow Z^n$ is an integer mapping from the n-dimensional space of real values to the n-dimensional space of integers. In this step, the mapping function S provides alternative options besides the ILS in Eq. (22), which covers various integer estimation methodologies. Prominent alternatives include integer bootstrap (IB) [24] and integer rounding (IR) [24]. Nonetheless, ILS stands out as the most efficacious among these approaches [25]. However, when ILS is used, the calculation can take a lot of time. The precision of the elements of the ambiguity vector can be increased, while simultaneously greatly reducing the correlation between ambiguities. This reparameterization is called Z-transformation, and it transforms the original DD ambiguities into a new set of ambiguities as follows [26]:

$$\hat{z} = Z^T \hat{a} \tag{27}$$

Where $\hat{a}$ is the estimation of a in the first step, Z is the transformation matrix and $\hat{z}$ is the new set of ambiguities. The corresponding covariance matrices are [27]:

$$Q_{\hat{z}\hat{z}} = Z^T Q_{\hat{a}\hat{a}} Z,\ \ Q_{\hat{b}\hat{z}} = Q_{\hat{b}\hat{a}} Z \tag{28}$$

An integer search is required to compute the ILS solution. After reparameterization, the search space is defined with the transformed ambiguities as follows [14]:

$$F(z) = (\hat{z} - z)^T Q_{\hat{z}\hat{z}}^{-1} (\hat{z} - z) \leq \chi^2, \quad z \in \mathbb{Z}^n \tag{29}$$

This search space is bounded by a hyper-ellipsoid, centered at zˆ, characterized by the covariance matrix $Q_{\hat{z}\hat{z}}$, and its dimensions determined by χ^2 . The application of the triangular decomposition of $Q_{\hat{z}\hat{z}}$, allows for the rewriting of the left-hand side of the quadratic inequality in Eq. (29) as a sum-of-weighted squares [19]:

$$\sum_{i=1}^{n} \frac{(\hat{z}_{i|I} - z_i)^2}{\sigma_{i|I}^2} \leq \chi^2 \tag{30}$$

The left side of the above equation corresponds to the conditional least-squares estimator, denoted as $\hat{z}_{i|I}$, which emerges when conditioning is applied to the integers z_i and $i = 1, 2, \ldots, n-1$. Employing the sum-of-squares format the subsequent step involves establishing n intervals for the search. These sequential intervals are defined as:

$$\begin{aligned} (\hat{z}_1 - z_1)^2 &\leq \sigma_1^2 \chi^2 \\ (\hat{z}_{2|1} - z_2)^2 &\leq \sigma_{2|1}^2 \left(\chi^2 - \frac{(\hat{z}_1 - z_1)^2}{\sigma_1^2}\right) \\ &\vdots \end{aligned} \tag{31}$$

Where $\sigma_i^2, i = 1,2,\ldots,n-1$are variance of i-th integer ambiguity. After this extensive integer estimation step, the fixed solution step will start. Here, the estimated integer ambiguities are employed to update the baseline vectors. The solution can be implemented directly as follows [14]:

$$\check{b} = \hat{b} - Q_{\hat{b}\hat{z}} Q_{\hat{z}\hat{z}}^{-1} (\hat{z} - \check{z}) \tag{32}$$

Where $\hat{b}$ is the float baseline vector, $\hat{z}$ is the transformed and float ambiguity vector, $\check{z}$ is the transformed and estimated true ambiguity vector and $\check{b}$ is the updated true baseline vector.

3.2 New Method

The method employed in this study can be categorized as search-based, as it seeks to determine the integer ambiguity within defined limits. However, selecting an appropriate limit can be a challenging task as it is crucial to balance computational burden and accuracy. Excessive computational costs may yield imprecise outcomes, while a narrow range may result in inaccuracies due to the potential exclusion of the correct solution. Therefore, careful consideration is essential when deciding on an appropriate search range to ensure that reliable and accurate results are obtained. To prevent this:

We are using only fractional parts of the carrier phases. Maximum of search area is around the L/λ [20].

Rotation constraints which are calculated by the IMU data [27] were added to pull the correct ambiguity from candidates.

The steps of the proposed method are as follows:

Step 1: Removal of the integer part of the DD carrier phase measurements

Thus, integer ambiguities will be in the range of the baseline length.

$$\nabla\Delta\widetilde{\emptyset} = \nabla\Delta\emptyset - \text{round}(\nabla\Delta\emptyset) \tag{33}$$

Here $\nabla\Delta\widetilde{\emptyset}$ is the fractional part of the DD carrier phase measurements and $\nabla\Delta\emptyset$ is the original carrier phase measurements.

Step 2: Candidate assignment.

The search area for any ambiguity is:

$$-\frac{L}{\lambda} < a_i < +\frac{L}{\lambda} \tag{34}$$

In this step candidate of integer ambiguities are assigned.

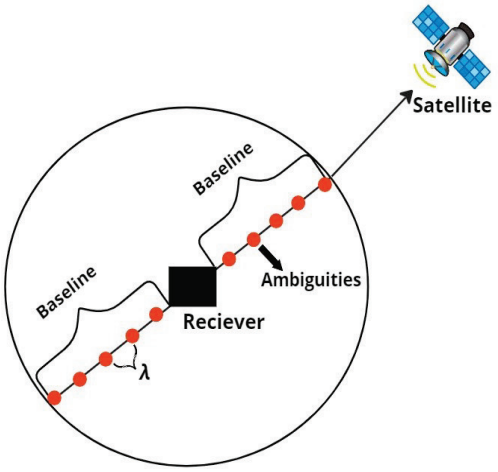

Figure 2 Diagram of possible ambiguities after fractional parts of DD carrier phases remain.

Step 3: Candidate base vectors.

For any candidate of a, the base vector is calculated using the LS method:

$$\hat{b}_j = (B^T R^{-1} B)^{-1} B^T R^{-1} (y - A\hat{a}_j), j = 1,2,\ldots,N_p \tag{35}$$

Where N_p is the number of total integer ambiguity candidates, R is the covariance matrix of DD carrier phase and pseudorange measurements. In the search step, instead of $\hat{a}$ in Eq. (34), all possible values shown in Fig. 2, are substituted one by one. For each of these candidate ambiguities, $\hat{b}_j(a)$ is calculated. When a low-cost GPS is used, the covariance of the base vector and integer ambiguity in float solution is high. Then when the search area is selected as shown in Step 2, the total number of candidates will reduce significantly. Although the number of candidates and the computational load have been reduced by taking fractional parts of the DD carrier phases, the number of candidates is still high due to the high error of low-cost GPSs. Therefore, it is reduced by adding constraint conditions to the candidate $\hat{b}(\hat{a})$.

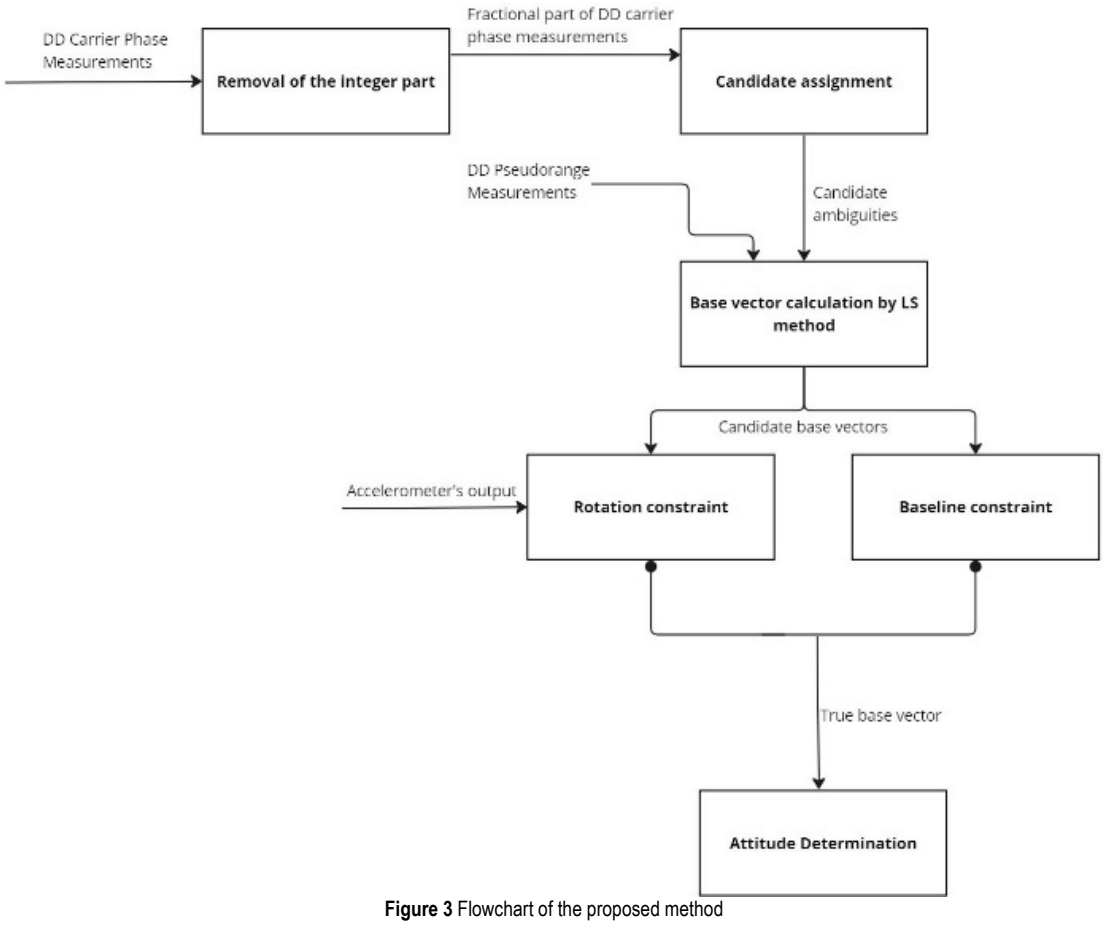

Figure 3 Flowchart of the proposed method

Baseline Constraint: In our case, the antennas remain stationary during rotation. Therefore, the baseline norm does not change. Then for sieving of candidates of the base vector, we can use the following constraint:

$$\ell - \delta\ell < \left|\hat{b}_j(a)\right| < \ell + \delta\ell \, , j = 1,2, \dots, N_p \tag{36}$$

Rotation constraint: Since the pitch angle is determined by accelerometers, it is compared by pitch angle determined by any base vector. When the error remains lower than a threshold, those candidates will be accepted.

$$\theta_a = \tan^{-1}\left(\frac{f_x}{\sqrt{(f_y)^2+(b_z)^2}}\right) \tag{37}$$

$$\theta_b = \tan^{-1}\left(\frac{b_z}{\sqrt{(b_y)^2+(b_x)^2}}\right) \tag{38}$$

Where f denotes the output of the accelerometer. Meanwhile, θ_a represents the pitch angle calculated by the accelerometer, and θ_b signifies the pitch angle calculated by the base vector. The threshold value is determined according to the difference of these two pitch angles.

$$|\theta_b - \theta_a| < \Delta\theta \tag{39}$$

The chart below depicts the flowchart of the proposed method.

4 ANALYSIS OF TESTS

This section includes the conditions for conducting the tests required to apply the methods mentioned in Section 3.2, the information on the materials used, and the analyses of the tests performed. Additionally, the results of the LAMBDA method and the new proposed method are compared.

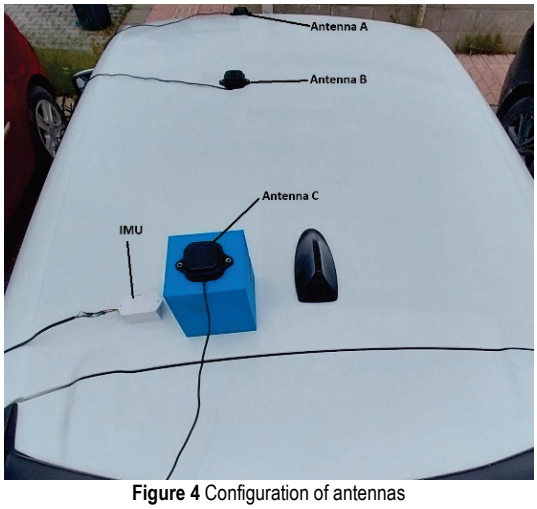

Figure 4 Configuration of antennas

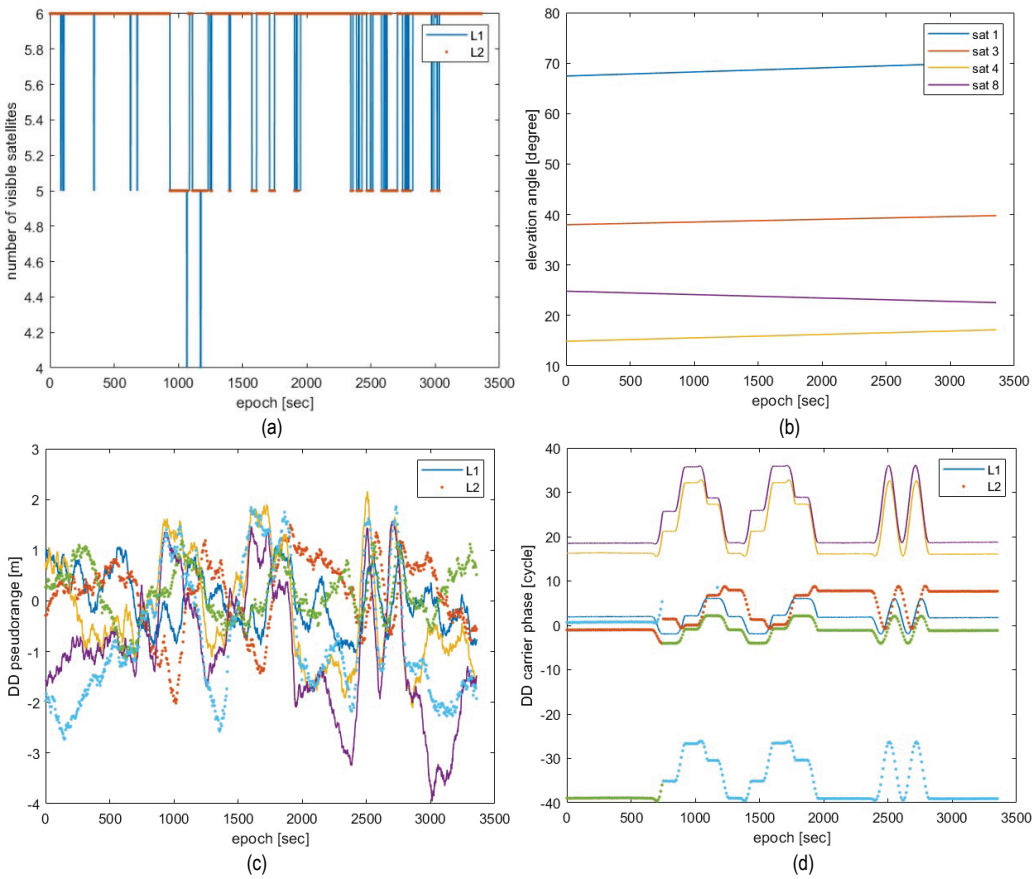

Figure 5 (a) number of visible satellites, (b) elevation angles of visible satellites, (c) DD pseudorange measurements, (d) DD carrier phase measurements.

The tests were conducted using a U-blox ZED-F9P GNSS receiver, an MPU-9255 IMU, and an STM32F407 electronic board. This electronic board was used to read data from four GNSS receivers and one IMU. The STM32CUBEIDE software was utilized to obtain the necessary data packets from the GNSS receivers and IMU mounted on the electronic board. After acquiring the data, the mentioned algorithms were implemented using MATLAB.

Moreover, this section includes graphs for visible satellites, elevation angles, pseudorange and carrier phase measurements, and rotation for both methods. Given that the test was conducted in a multipath environment, only satellites with elevation angles exceeding 10 degrees were processed to mitigate multipath errors, resulting in a low number of visible satellites. The measurements and the count of visible satellites are presented separately for the L1 band.

The test was conducted with a baseline length of 0.75 meters and a fixed pitch angle of 20 degrees throughout. The system's X direction was initially aligned with the north direction, and the vehicle underwent a complete rotation, turning 90 degrees west, 90 degrees south, 90 degrees east, and finally returning to the north direction. Subsequently, another full circle was completed, this time without any stops, moving from north to north.

As seen in Fig. 5a, the number of visible satellites varies during the test as the vehicle moves. Although the maximum visible satellite count is 6, only 4 satellites are selected from each band because 4 of these satellites have elevation angles greater than 10 degrees. Since the suitable satellites for both the L1 and L2 bands are the same, their elevation angles are identical. We previously mentioned that pseudorange measurements are noisy and misleading, as observed in Fig. 5c, while sudden changes in measurements due to integer ambiguities in carrier phases are seen in Fig. 5d. Additionally, carrier phase noise is minimal.

Due to the high error of the receivers, when estimating rotation using the LAMBDA method, as depicted in Figs. 6a and 6c, the pitch angle exhibits notably poor accuracy. Furthermore, within Figs. 6d and 6e, trajectory graphs depict the base vector corrected using both the LAMBDA and New methods. In the New method, the base vector closely approximates the norm value of 0.75 meters. However, discrepancies are evident in the LAMBDA method, manifesting as errors.

Table 1 Methods and mean error values (degree)

	0.75 meter baseline
LAMBDA	Heading: 30 deg Pitch: 40 deg
New Method	Heading: 3 deg Pitch: 5 deg

In Tab. 1, the mean error values of heading and pitch angles for two separate methods are given. As can be seen, our method is much more successful than the LAMBDA method. The LAMBDA method gives poor results, especially in multipath conditions with few satellites.

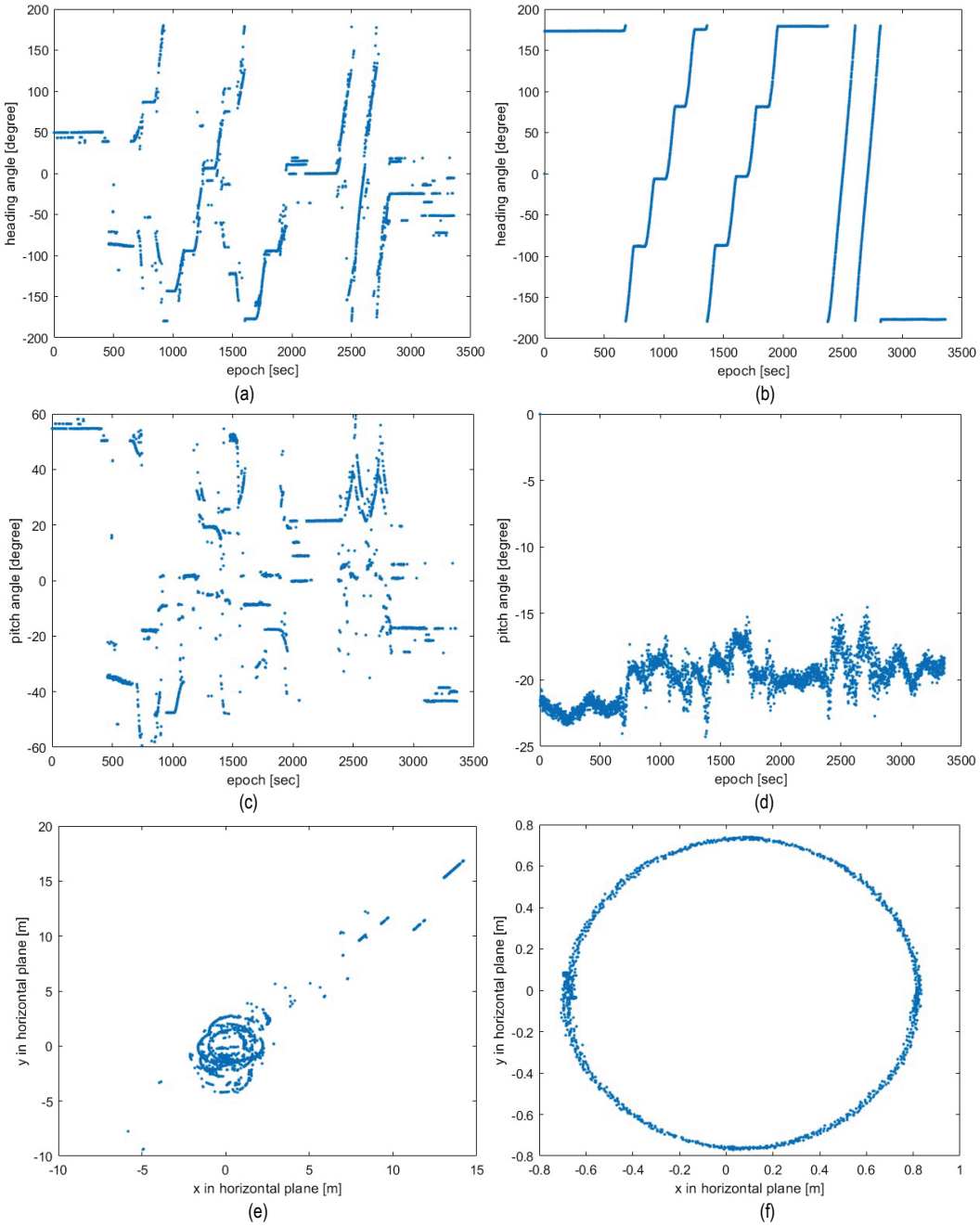

Figure 6 (a) heading angle by LAMBDA method, (b) heading angle by New method, (c) pitch angle by LAMBDA method, (d) pitch angle by New method, (e) fixed trajectory by LAMBDA method, (f) fixed trajectory by New method

5 CONCLUSIONS

In this study, a comparison between the LAMBDA method and the new method in detecting and correcting integer ambiguities in carrier phases was conducted. While the LAMBDA method is widely used in carrier phase applications, it exhibits poor performance, especially in environments prone to multipath effects. On the other hand, the new method, incorporating baseline and rotation constraints, demonstrates superior performance even in challenging multipath-rich environments.

In the conducted tests, the new method consistently outperforms the LAMBDA method, showing significantly reduced mean error values in heading and pitch angles. This improvement is particularly noteworthy considering the adverse conditions tested, which included multipath effects from buildings, trees, and vehicles. Moreover, even with antennas and receivers exhibiting elevated error rates, the new method still demonstrates considerable accuracy improvements.

The potential of the new method could be further enhanced, particularly in environments free from multipath interference, such as those achievable with drones or aircraft. Additionally, employing more precise antennas and receivers could lead to even better results.

6 REFERENCES

[1] Subirana, J. S., Zornoza, J., & Hernández-Pajares, M. (2013). *GNSS data processing: Fundamentals and algorithms*. European Space Agency.

[2] Buist, P. J. (2007). The baseline constrained LAMBDA method for single epoch, single frequency attitude determination applications. In *Proceedings of the 20th International Technical Meeting of the Satellite Division of the Institute of Navigation (ION GNSS)* (pp. 2962–2973).

[3] Fan, S., Zhang, K., & Wu, F. (2005). Ambiguity resolution in GPS-based, low-cost attitude determination. *Journal of Global Positioning Systems, 4*(1–2), 207–214. https://doi.org/10.5081/jgps.4.1.207

[4] Hatch, R. (1991). Instantaneous ambiguity resolution. In *Kinematic systems in geodesy, surveying, and remote sensing: Symposium No. 107* (pp. 299–308). Springer. https://doi.org/10.1007/978-1-4612-3102-8_27

[5] Chen, D. (1993). Fast ambiguity search filter (FASF): A novel concept for GPS ambiguity resolution. In *Proceedings of the 6th International Technical Meeting of the Satellite Division of the Institute of Navigation (ION GPS)* (pp. 781–787). Salt Lake City, UT.

[6] Counselman, C. C., & Gourevitch, S. A. (1981). Miniature interferometer terminals for Earth surveying: Ambiguity and multipath with global positioning system. *IEEE Transactions on Geoscience and Remote Sensing, GE-19*(4), 244–252. https://doi.org/10.1109/TGRS.1981.350379

[7] Lu, G. (1995). *Development of a GPS multi-antenna system for attitude determination* (Master's thesis). University of Calgary, Calgary, Canada.

[8] Kim, D., & Langley, R. B. (1999). An optimized least-squares technique for improving ambiguity resolution and computational efficiency. In *Proceedings of the 12th International Technical Meeting of the Satellite Division of the Institute of Navigation (ION GPS)* (pp. 1579–1588). Nashville.

[9] Wang, Y., Zhan, X., & Zhang, Y. (2007). Improved ambiguity function method based on analytical resolution for GPS attitude determination. *Measurement Science and Technology, 18*(9), 2985–2990. https://doi.org/10.1088/0957-0233/18/9/032

[10] Han, S., & Rizos, C. (1996). Improving the computational efficiency of the ambiguity function algorithm. *Journal of Geodesy, 70*(6), 330–341. https://doi.org/10.1007/BF00868185

[11] Erickson, C. (1992). *Investigations of C/A code and carrier measurements and techniques for rapid static GPS surveys* (Master's thesis). University of Calgary, Calgary, Canada.

[12] Park, C., Kim, I., Lee, J. G., & Jee, G. (1996). Efficient ambiguity resolution using constraint equation. In *Proceedings of Position, Location and Navigation Symposium - PLANS '96* (pp. 277–284). IEEE. https://doi.org/10.1109/PLANS.1996.509089

[13] Teunissen, P. J. G. (1994). A new method for fast carrier phase ambiguity estimation. In *Proceedings of 1994 IEEE Position, Location and Navigation Symposium - PLANS'94* (pp. 562–573). IEEE. https://doi.org/10.1109/PLANS.1994.303362

[14] Verhagen, S., & Li, B. (2012). *LAMBDA software package: MATLAB implementation* (Version 3.0). Perth, Australia.

[15] Bejeryd, J. (2007). *GPS-based attitude determination*. Institutionen för systemteknik, Linköping.

[16] Ma, L., Zhu, F., Liu, W., Lu, L., Lou, Y., & Zhang, X. (2022). VC-LAMBDA: A baseline vector constrained LAMBDA method for integer least-squares estimation. *Journal of Geodesy, 96*(9), 59. https://doi.org/10.1007/s00190-022-01644-7

[17] Liu, X., Chen, G., Zhang, Q., & Zhang, S. (2017). Improved single-epoch single-frequency PAR LAMBDA algorithm with baseline constraints for the BeiDou navigation satellite system. *IET Radar, Sonar & Navigation, 11*(10), 1549–1557. https://doi.org/10.1049/iet-rsn.2017.0048

[18] Teunissen, P. J. G. (2010). Integer least-squares theory for the GNSS compass. *Journal of Geodesy, 84*(7), 433–447. https://doi.org/10.1007/s00190-010-0380-8

[19] Park, C., & Teunissen, P. J. G. (2009). Integer least squares with quadratic equality constraints and its application to GNSS attitude determination systems. *International Journal of Control, Automation and Systems, 7*(4), 566–576. https://doi.org/10.1007/s12555-009-0408-0

[20] Li, W., Fan, P., Cui, X., Zhao, S., Ma, T., & Lu, M. (2018). A low-cost INS-integratable GNSS ultra-short baseline attitude determination system. *Sensors, 18*(7), 2114. https://doi.org/10.3390/s18072114

[21] Shoemake, K. (1994). Euler angle conversion. In *Graphics Gems* (pp. 222–229). https://doi.org/10.1016/B978-0-12-336156-1.50030-6

[22] Sidi, M. J. (1997). *Spacecraft dynamics and control: A practical engineering approach* (Vol. 7). Cambridge University Press.

[23] Ghanbarpour, A. H., Pourtakdoust, S. H., & Samani, M. (2009). A new non-linear algorithm for complete pre-flight calibration of magnetometers in the geomagnetic field domain. *Proceedings of the Institution of Mechanical Engineers, Part G: Journal of Aerospace Engineering, 223*(6), 729–739.

[24] Teunissen, P. J. G. (1998). Success probability of integer GPS ambiguity rounding and bootstrapping. *Journal of Geodesy, 72*, 606–612. https://doi.org/10.1007/s001900050199

[25] Teunissen, P. J. G. (1999). An optimality property of the integer least-squares estimator. *Journal of Geodesy, 73*(11), 587–593. https://doi.org/10.1007/s001900050269

[26] De Jonge, P., & Tiberius, C. (1998). *The LAMBDA method for integer ambiguity estimation: Implementation aspects* (Publications of the Delft Geodetic Computing Center, No. 12).

[27] Eling, C., Klingbeil, L., & Kuhlmann, H. (2015). Real-time single-frequency GPS/MEMS-IMU attitude determination of lightweight UAVs. *Sensors, 15*(10), 26212–26235.

Authors' contacts:

Habib Kanberoğlu (Habib Ghanbarpourasl)
(Corresponding author)
Department of Computer Engineering,
Turkish Aeronautical Association University,
Bahçekapı Mahallesi Okul Sk. No: 11, 06790 Etimesgut-Ankara, Turkey
hghanbarpourasl@thk.edu.tr

Mukaddes Bolat
Department of Mechanical and Aeronautical Engineering,
Turkish Aeronautical Association University,
Bahçekapı Mahallesi Okul Sk. No: 11, 06790 Etimesgut-Ankara, Turkey